Infrared Beam Combining and Detection

Stephen T. Ridgway
NOAO/KPNO, P.O. Box 26732, Tucson, AZ 85726

L.1. PURPOSE OF THE BEAM COMBINER/DETECTOR SUBSYSTEM

In order to obtain interferometric measures, the multiple telescope beams must be combined with equal optical paths. The infrared and optical beam combiner subsystems each receive the seven telescope beams, form the optical combinations (analogous to the correlator in a radio interferometer), and detect the interference fringe amplitudes and relative phases.

L.2. REQUIREMENTS

The beam combiner should detect as much as possible of the information contained in the 21 complex amplitudes which describe the accessible $u - v$ points for each observing configuration. It should have sensitivity and noise performance which are consistent with achieving the highest priority CHARA science goals.

Initially, the highest science priority for the infrared configuration of CHARA will be the study of YSO's. The bright T Tauri stars in nearby star formation regions have V magnitudes of 8–12 and K magnitudes of 6–10.

The most important wavelengths are 2.1–2.4 microns. Near these wavelengths YSO's show spectral features associated with the stellar surface, accretion disk and boundary layer, dust envelope, and the gaseous material between. The system can probably be optimized over the range 1.5–2.5 μm without much compromise of the performance in the 2.1–2.4 μm region. It may be possible to extend operation closer to 1 μm as well.

The beam combiner should be stable. It should not require more than minor realignment over a time-scale of days, and not at all during a night. Drifts in visibility and phase should be negligible during typical observing cycles of 15–30 minutes. The initial configuration of the infrared beam combiner should require only demonstrated technology and should be available at first-light. There should be an upgrade path for the beam combiner, which may require further technical development or R&D.

L.3. OPTICAL PATH DIFFERENCE TRACKING

In photon limited interferometry, it is advantageous to record the interferometric signal with high time resolution. Consequently, the signal may be used to provide OPD information with no loss of sensitivity. In that case, it is sufficient to keep the OPD within a range which maintains high visibility. The photon limited case applies with some visible wavelength detectors.

In the faint limit, the infrared detectors are strongly limited by detector noise. When detector noise is the limiting noise source, the situation is complex. There are several possible strategies for path difference tracking. If the OPD can be stabilized, then the

signal can be integrated, and the S/N increases linearly with time until detection is out of the detector noise regime. However, stabilizing the OPD requires a separate, fast fringe detection system.

The most attractive option is to use the visible signal (typically 0.5–1.0 μm) to stabilize the OPD, and then integrate with the noisier infrared detector. This approach is rendered difficult owing to dispersion between IR and visible — the infrared fringes occur for a different OPD than for the visible. However, the IR increased sensitivity and dynamic range of this method motivates considerable additional effort to implement it.

A second strategy is to select the integration time to be just fast enough to "freeze" the atmospheric fluctuations. The OPD error signal can be determined from the most recent data, and can then be used to keep the OPD within the high visibility tolerance, without actually stabilizing the OPD sufficient for long integrations. Unfortunately, rapid readout of the detector arrays results in even more severe noise.

A third strategy is to develop an infrared OPD detector separate from the science detector. A very interesting approach would be to use germanium photodetectors or avalanche photodiodes. These detectors have high QE and their peak sensitivity is in the range 0.8–1.6 microns, which is well suited for fringe tracking for both visible and infrared beam combiners. However, the detector technology is not yet sufficiently advanced to specify these detectors for the first-light beam combiners.

L.4. REVIEW OF BEAM COMBINER DESIGNS

The options for infrared beam combiner design are similar to the options for visible beam combiners. A number of these are described in Appendix K. Refer to this section for discussions of these concepts.

The infrared implications are more complex in several respects. The detectors are limited more strongly by detector noise than CCD's. Also, some measurements, especially large optical bandwidth and long integrations, may be limited by thermal background noise, especially at wavelengths beyond about 2.3 microns.

L.4.1. Required Bandwidth and Resolution

For a Kolmogoroff turbulence spectrum characterized by the Fried parameter r_0, the RMS phase difference $\delta\Phi_{RMS}$ in waves expected between two telescopes separated by δx is (Beckers 1991),

$$\delta\Phi_{RMS} = 0.42(\frac{\delta x}{r_0})^{\frac{5}{6}}. \tag{L.1}$$

or less for a finite outer scale of turbulence.

In order to find the fringes (OPD location) with some facility, it is reasonable to require that the fringe coherence length should be at least equal to $\delta\Phi_{RMS}$. The coherence length in waves is the spectral resolution R, so we require a resolution,

$$R \geq 0.42(\frac{\delta x}{r_0})^{\frac{5}{6}}. \tag{L.2}$$

Under conditions of 1.″0 seeing at 0.5 μm, this imposes the following requirements for R:

δx	R(0.5 μm)	R(2.2 μm)
100 m	133	30
350 m	377	86

While the resolution might be relaxed if the fringes are tracked with a separate fringe tracker system, in the following we will require R=100 at 2.2 microns, or a resolution element of 0.022 μm = 220 nm. Over the spectral range 2.0–2.5 microns, there will be 23 resolution elements, requiring 46 data points (pixels) for minimal sampling.

L.4.2. Detector Noise

Single element InSb detectors have been used for more than a decade in infrared astronomy. Equipped with the standard transimpedance amplifier, these have typical noise equivalent power (NEP) at frequencies of a few $\times 10^2$ Hz of about $1 \times 10^{-14}\ W/\sqrt{Hz}$. This is equivalent to a readout noise of $1 \times 10^5\ e^-$ for a time constant of 1 sec.

It has been reported that similar detectors equipped with charge coupled amplifiers can operate with read noise of 300 e^- (Di Benedetto et al. 1992). This is likely to be limited to low readout rates.

The first generation of widely used infrared detector arrays, the 58×62 InSb arrays, have a readout noise of about 300 e^- , while the current 256×256 products have a read noise of about 30 e^- (Santa Barbara Research Corporation). These are independent of integration time, provided there is sufficient time for the multiple reads employed to reduce the effect of correlated noise (effectively to suppress the 1/f noise in the readout circuit).

In the following discussion, we will assume that discrete InSb detectors have a read noise of 300 e^- and that array detectors have a read noise of 30 e^- for "slow" readout and 100e^- for "fast" readout.

L.4.3. Thermal Background Noise

Thermal background becomes important in this instrument for wavelengths longer than about 2.3 μm. The magnitude of the background is a sensitive function of the cold baffling, which will be very design dependent in some of the the multi-beam combiners.

The simplest case is the on-axis combiner in which the detector sees a superposition of the seven apertures. We assume here an effective image width of 1 arcsecond.

In the off-axis combiners, the background will be at least 7$\times$ greater, since the multiple pupils are not superimposed at the cold stops.

For bandwidth 0.011 μm and aperture of one arcsecond, with an effective emissivity of 1.0 at T=283 K the thermal flux is approximately 5 photons/sec (negligible) at 2.3 μm. At 2.5 μm the flux has increased to 3600 photons/sec. After one second integration the noise associated with background would be $\sqrt{3600\eta}$, where η is the efficiency. Hence thermal background is significant only at the red end of the 2.0–2.5 μm region.

In the case of fiber coupled detection, the baffling will be less optimal (the fiber will be

oversize and there will be some loss of flux concentration). For an approximate comparison of the options, we will assume that each fiber has a projected diameter on the sky of $3''$.

L.5. FIGURE OF MERIT

The figure of merit described for the visible beam combiner is modified for the infrared case.

$$M = \frac{0.99^R \times 0.95^T \times B}{N_{conf} \times S} \tag{L.3}$$

Here, the reflections are assumed to be more efficient than in the visible, in accordance with the characteristics of high quality silver coatings. B is again the optical bandwidth, which is reduced for detection without spectral dispersion. N_{conf} is the number of configurations required to obtain all of the image visibilties.

S is the noise in the observation. In the case of detector noise, $S = \sqrt{N_{det}} R_n$, where N_{det} is the number of detectors or pixels contributing noise and R_n is the noise for a single detector or pixel. In the case of background limited performance, S is simply the background associated noise.

The detector quantum efficiency is not included here as both discrete and array InSb detectors have similar DQE of about 80% (if anti-reflection coated).

We will compare a number of concepts, including all of the ones described for the visible image system, as well as the concept recommended here and some variants on these. For example, note that the on-axis (pupil plane) combiners can be operated with discrete detectors and a reduced bandwidth, or with dispersion and an array detector.

It is important to note that the number of configurations required to detect all the closure phases is larger than the number required to detect the visibilities. If this factor is considered, then the 7-beam non-redundant techniques gain an additional advantage of approximately $4\times$ in the merit factor for full imaging operation only. For this reason, an early upgrade to one of these concepts is intended.

An additional column of merit factors can be computed for the background noise limited case, but since this only applies to the few reddest spectral channels it will not be considered further here.

As in the visible case, we find a clear advantage for the concepts which combine all beams simultaneously. As with the visible case, the 7-Beam Non-Redundant 1D case presents formidable problems of implementation, even more severe in the infrared since the large collecting optic greatly complicates the requirement to maintain low thermal background on the detectors. The 7-Pair Fiber Coupled concept requires only multimode fibers, but retains a relatively high merit factor.

The Optical fiber-fed Non-Redundant approach requires single mode optical fibers. Until recently these were not commercially available. However, the Verre Fluoré company in France, aided by a technology development grant, has worked closely with astronomers in recent years (Foresto et. al. 1993), to develop single mode zirconium fluoride fibers for interferometry. The availability as a commercial product was recently announced (Physics Today, Dec. 1993), and we now feel justified in planning to use these fibers with the CHARA Array. The existing fibers are adequate for an initial implementation, and work is continuing at Verre Fluoré on products with improved characteristics. In view of the

TABLE L.1. Comparison of beam combiner schemes.

Beam Combiner Scheme	N_{conf}	R	T	B	N_{det}	R_N	M
3-way combination	5	2	3	220	14	300	0.032
same – fiber-coupled, dispersed on array	5	2	5	5000	644	30/300	0.98/0.32
All beams	1	4	4	220	8	300	0.19
4-beam non-redundant 1D	7	6	4	5000	552	30/300	0.73/0.24
7-beam non-redundant 1D	1	5	3	5000	1932	30/300	2.94/0.97
7-beam non-redundant 2D	1	8	3	220	100	30/300	0.66/0.22
7-beam optical fiber-fed non-redundant 1D	1	0	6	5000	1932	30/300	2.79/0.92
7-pair	4	1	6	220	14	300	0.04
same – fiber-coupled, dispersed on array	4	1	8	5000	644	30/300	1.07/0.35

Notes to table: The number of detectors corresponds to just the number of discrete detectors for non-dispersed detection, or for dispersed detection to the number of pixels in an array with dimensions 46 (required for spectral resolution 2.0–2.5 μm) by the number of pixels corresponding to the number of beams if spatially separated, or to the number of pixels required to resolve spatial frequency encoding for the number of beams combined. For the 7-Beam Non-redundant 2D, the number corresponds to 10×10, required to resolve the 2D spatial frequencies.

Where there are two entries for the noise and figure of merit, these correspond to the assumptions of slow array readout (low noise) or fast array readout (higher noise).

relatively high merit factor and moderate cost, the 7-beam optical fiber-fed non-redundant 1D combiner is our selection for the infrared.

L.6. DESIGN OF THE INFRARED BEAM COMBINER

L.6.1. The Optical Layout

The IR beam combination/fringe tracker system begins with the pickoff mirrors/dichroics which divert the seven telescope beams onto the IR table. Several commercial dichroic coatings are availabe, as well as the old standby, a thin gold layer. In order to switch the dichroics in and out of the beam, the entire row of mounts, fixed on a single platform, can be removed, either by hand (kinematic replacement) or remotely (with a motorized precision slider mechanism).

The beams then enter short optical delay lines. These delay lines appear as circles in the diagram, as the proposed implementation is to divert each beam upward from the table into a catseye, then to return it to the axis of propagation.

These delay lines are required in order to use the full spectral bandwidth of the visible fringe tracking system. The atmospheric dispersion correction for the visible beams introduces a net OPD shift for each beam. These must be compensated in the infrared beams in order to use visible fringe tracking with infrared imaging. This must be done after the dichroics separating visible/infrared flux, and before the beam combiner. The short delay lines could be dispensed with if only the red end of the silicon spectral range is used, and for short baselines. However, we expect that the use of visible fringe tracking for infrared imaging will be a powerful technique and we plan to use it extensively.

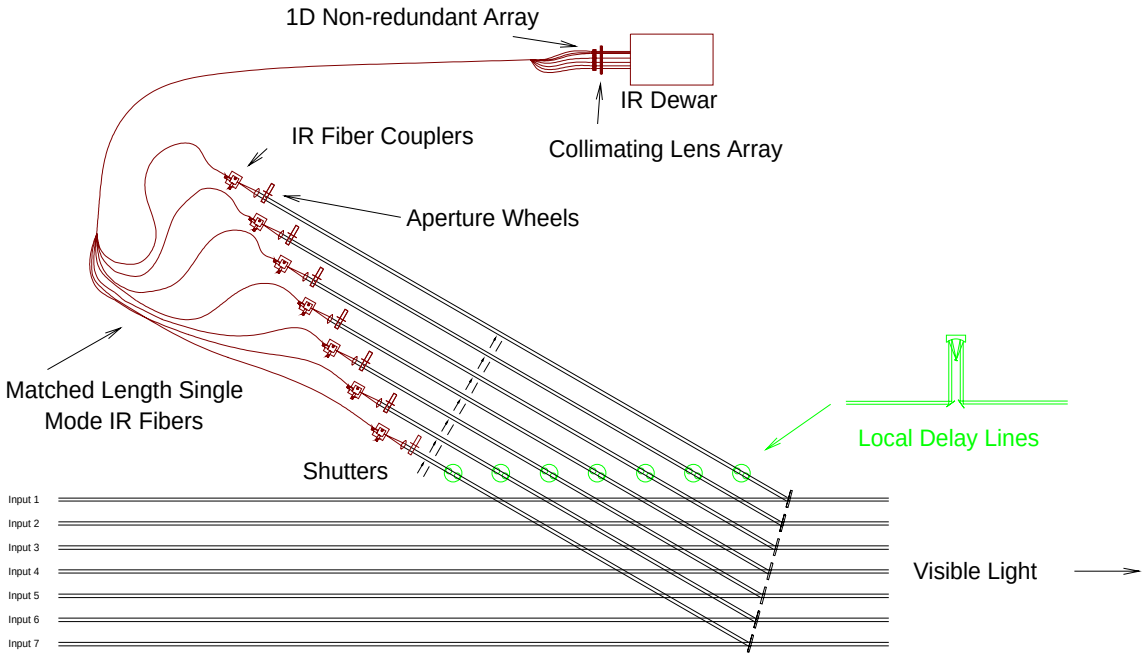

FIGURE L.1. Seven-pair combiner with fiber coupling and dispersion onto an array detector.

Lenses focus the beams onto seven fiber ends. Each fiber injection lens should be assembled in a common fixture with its fiber. The fiber tip should have fine adjustment in focus and (x, y) position. Exceptional stability is required for these components. For initial adjustment, there will be an alignment unit which can be inserted in front of the lens. This unit will consist of a visible beamsplitter, a corner cube, and a small video camera.

The optical fibers are single mode fibers, which conduct the light to the detector in a 1D, non-redundant configuration. This is completely analagous to the imaging section of the visible beam combiner. Fiber ends in the array will be reimaged onto a homologous array of apertures at a cold stop in the IR detector system. Following the apertures the diverging beams will be collimated and passed through a grism to provide low spectral resolution.

The most promising detectors for the 1–2.5 μm spectral region are InSb or HgCdTe detectors. Both require cryogenic cooling in order to reduce the photon flux from thermal background emission. That is, the detector must be in an enclosed cold chamber which only 'sees' the warm exterior through an opening which is carefully baffled with cold filters and apertures. InSb requires a temperature around 40 K, i.e. a little cooler than LN2, usually achieved with LHe liquid or cryo-coolers. HgCdTe can function with just LN2 cooling, since its responsivity drops off at wavelengths beyond 2.5 microns. This will probably be the preferred option.

There will be a test-alignment source, consisting of a tungsten filament bulb producing both visible and IR flux which will propagate in reverse through the fibers and into the interferometer.

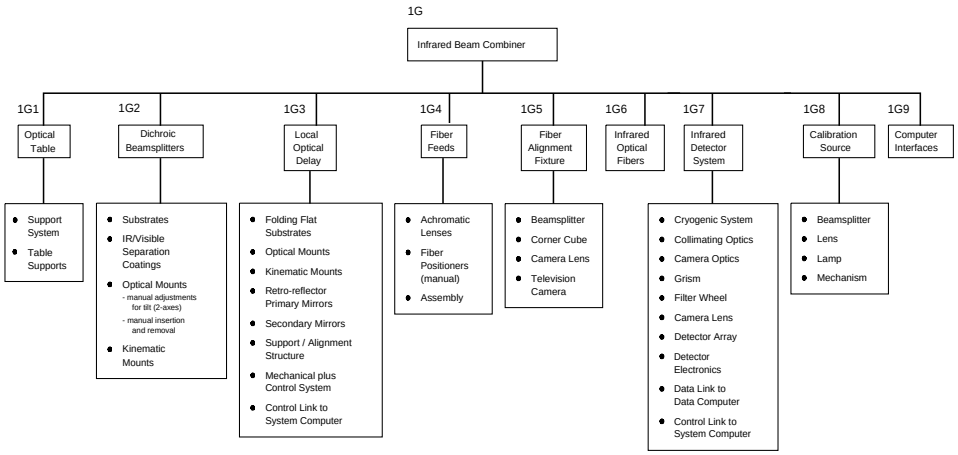

FIGURE L.2. Hardware tree for the infrared beam combiner.

L.6.2. Discussion of the Concept

The proposed beam combiner has the advantage of few components. It produces all image information which the telescopes can deliver, 21 visibilities and 35 closure phases, in a single exposure. The only difficult feature of this concept is injecting the light into the single mode fiber. Exceptionally stable components will be employed, and in performance computations a relatively low injection efficiency of 30% is assumed, although theoretical values approach 70%.

L.7. HARDWARE TREE AND COST

A hardware tree describing the major assemblies in the IR Beam Combiner is shown in Figure L.2.

A detailed cost study indicates that most of the components for the IR beam combiner concept described here can be acquired from commercial sources as standard products. Specific cost information is summarized elsewhere in this report.

L.8. THE INFRARED DETECTOR

The IR detector will consist of the actual array with its accompanying cryogenic system and electronics. Although closed cycle coolers are available, they generate vibrations which are likely to be excessive in the interferometric lab. Therefore a liquid cryogen reservoir is preferred. The cryogenic volume will also contain some optics which must be cold to preserve the sensitivity of the detector. The cryogenic work space is likely to occupy about 0.5 cubic foot.

The detector electronics will normally be closely coupled to a supporting computer system. Control signals will be transmitted to the detector electronics, and data will be returned. The data rate will consist of images, up to as large as 256×256 by 2 bytes deep, but most likely a sub-raster will be sufficient, possibly as small as about 50×50. With the sub-raster read, a frame rate of at least 100 Hz may be required (e.g. for observation of IR sources

with no visible counterpart). In order to maintain the frame rate, it may be necessary to carry out some data compression in the dedicated detector electronics.

The detector will have two operating modes. In IR-passive mode, the fringes will be stabilized with reference to the signals detected in the visible beam combiner. The IR detector will be simply a data acquisition device, recording and logging images for later reduction.

In the IR-active mode, a rapid image readout will be used to determine the fringe position and to return a fringe error signal to the fringe tracking system. It is probably not possible to lock fringes to a fraction of a wave with this system. More likely it will function as a slow fringe tracker, ensuring that the OPLE's stay within the coherence length of the beam combiner. For example, with the IR detector operating at a frame rate of 100 Hz, the fringe error signal returned to the fringe tracker servo would be updated at this rate. Thus this error signal (a few bytes) must be communicated to the fringe tracker control computer with minimal overhead.

L.9. RISKS

The dichroics are standard commercial products. We have tested a candidate commercial scanning stage (Anorad) which is satisfactory for the short optical delay lines.

We have extensive experience with the infrared single mode fibers (Foresto & Ridgway 1993), which are now a commercial product. The use of these remains a relatively difficult task. At GSU a fiber lab is now in operation, currently working with single mode quartz fibers for the visible. This work will be extended to the infrared at a future date.

L.10. REFERENCES

Beckers, J.M. 1991, *Exp. Astr.* **2**, 57

Di Benedetto, G.P., Braun, R., Foy, R. Genzel, R., Eckart, A., Koechlin, L., Mariotti, J.-M., & Weigelt, G., *Coherent Combined Instrumentation for the VLT Interferometer*, VLT Report No. 65, ESO, Garching, 1992)

Foresto, V. & Ridgway, S.T. 1993, in *High Resolution Imaging by Interferometry II*, ed. F. Merkle, (ESO, Garching) in press)

Foresto, V., Maze, G., & Ridgway, S.T. 1993, in *Fiber Optics in Astronomy II*, P. Gray, ed., PASP Conference Series, in press